Physicochemical Characterisation of Nanoporous Hydroxyapatite Doped with *Chromolaena odorata* Derived Polyphenols

Mangalagowri Sangar[a], Nur Farahiyah Mohammad[a,b,], Siti Shuhadah Md Saleh[c,d], Nor Shafiqah Mohamad Hanifah[a], Nashrul Fazli Mohd Nasir[a,b], Khairul Farihan Kasim[c], and Farah Diana Mohd Daud[e]

[a]Faculty of Electronic Engineering & Technology, Universiti Malaysia Perlis, Pauh Putra, 02600 Arau, Perlis, Malaysia
[b]Medical Device and Life Science Cluster, Sport Engineering Research Centre (SERC), Universiti Malaysia Perlis, Pauh Putra, 02600 Arau, Perlis, Malaysia
[c]Faculty of Chemical Engineering & Technology, Universiti Malaysia Perlis, Jejawi 2, 02600 Arau, Perlis, Malaysia
[d]Biomedical and Nanotechnology Research Group, Centre of Excellence Geopolymer and Green Technology (CEGeoTech), Universiti Malaysia Perlis, Jejawi, 02600 Arau, Perlis, Malaysia
[e]Manufacturing and Materials Engineering Department, Kuliyyah Engineering, International Islamic University Malaysia (IIUM), Jalan Gombak, 53100 Kuala Lumpur, Malaysia
*Corresponding author: farahiyah@unimap.edu.my

Abstract

The development of hydroxyapatite (HA) substituted with natural compounds from plants with antibacterial properties could be the solution for implant infections. In this study, the antimicrobial properties of nanoporous HA doped with polyphenols extracted from *Chromolaena odorata (C. odorata)* against *Staphylococcus aureus (S. aureus)* were evaluated. The polyphenolic compounds in both extracts were investigated based on the total phenolic content (TPC), total flavonoid content (TFC), and antioxidant activity. The results showed that 80% methanol *C. odorata* extract has 114.51 ± 4.63 mg GAE/g of TPC and 216.32 ± 3.98 mg QE/g of TFC. For 80% ethanol *C. odorata* extract, the TPC is 58.68 ± 3.67 mg GAE/g and the TFC is 61.84 ± 2.13 mg QE/g. Both 80% methanol and 80% ethanol extracts exhibited high antioxidant activity of 88.94% and 73.54%, respectively. The X-ray diffraction (XRD) analysis of the synthesised HA powder revealed three main peaks at $2\theta = 25.95°$, $32.01°$, and $33.03°$, corresponding to the diffraction planes of (002), (211), and (300), respectively. The Fourier transform infrared (FTIR) spectroscopy of HA-doped *C. odorata* extract indicated a reduction in the peaks for PO_4^{3-}, OH^-, CH, and CO_3^{2-} functional groups. The antimicrobial activity of HA-doped *C. odorata* pellets was investigated using the agar diffusion method, whereby the inhibition zones were 48 mm^2 and 106 mm^2 for concentrations of 20 mg/mL and 80 mg/mL, respectively. In conclusion, this study demonstrates the antimicrobial activity of HA doped *C. odorata* extract against *Staphylococcus aureus (S. aureus)* bacteria.

Keywords: Hydroxyapatite, Antimicrobial, Polyphenols, *Chromolaena odorata, Staphylococcus aureus*

Introduction

Bioceramic materials have become essential in modern medical and dental practices, offering versatile solutions for the repair and regeneration of bone and dental tissues [1],[2]. These materials are meticulously engineered to mimic the structural and functional characteristics of natural tissues, facilitating seamless integration with biological systems. Hydroxyapatite (HA), a leading bioceramic, holds particular prominence due to its striking resemblance to the mineral composition of bones and hard tissues, predominantly consisting of calcium phosphate compounds [3],[4]. This structural similarity enables HA to not only provide mechanical support but also to promote essential biological responses crucial for tissue regeneration and healing processes at the implant site [5]. When used in biomedical applications, HA establishes intimate interfaces with surrounding tissues, facilitating osseointegration in bone implants and biocompatibility in dental restorations [6]. Its bioactive properties not only stimulate bone cell activity but also contribute to the long-term stability and functionality of implants [7]. Moreover, the ability of hydroxyapatite (HA) to undergo controlled biodegradation concurrent with new tissue development emphasizes its effectiveness for stable integration into host tissues, positioning it as a critical material in regenerative medicine applications [8]. Despite their success, bioceramic implants are susceptible to post-implant infections, which can impair bone healing, cause significant bone loss, and lead to implant failure or even surgical intervention like amputation [9]. *Staphylococcus aureus (S. aureus)* is a common pathogen associated with implant infections [10], highlighting the urgent need for

effective antimicrobial strategies. Traditional antibiotics, while effective, face challenges due to the rise of antibiotic-resistant bacteria resulting from their widespread use [9].

Chromolaena odorata (C. odorata), commonly known as *Pokok Kapal Terbang*, is well-recognized for its potent antioxidant properties that facilitate wound healing [9],[10]. Extensive research has highlighted its diverse biological activities, including antibacterial, antifungal, antitumor, and anti-inflammatory effects, which collectively contribute to its therapeutic potential [11]. *C. odorata* contains a rich reservoir of bioactive compounds, prominently including polyphenols such as flavonoids and phenolic acids [11]. Previous study suggests that *C. odorata* has been demonstrating effectiveness against various pathogens, including bacteria and fungi [5],[6]. This antimicrobial action is attributed to its ability to disrupt microbial cell membranes, inhibit enzyme activity crucial for microbial survival, and interfere with microbial biofilm formation [6]. In addition to its antimicrobial properties, *C. odorata* exhibits remarkable antioxidant effects due to the presence of flavonoids and phenolic acids, which scavenge free radicals and mitigate oxidative stress [11]. This antioxidant activity not only supports wound healing processes but also enhances the overall biocompatibility of biomaterials in biomedical applications.

The anti-inflammatory potential of *Chromolaena odorata* (*C. odorata*) has also been extensively investigated, highlighting its relevance in implantology. By modulating inflammatory responses, *C. odorata* extracts can attenuate the inflammatory cascade associated with implantation procedures, thereby promoting accelerated healing and reducing the risk of complications such as infection and implant rejection [6]. The integration of *C. odorata* extract into bioceramic matrices, particularly hydroxyapatite (HA), capitalizes on these therapeutic properties to develop advanced biomaterials. Doping HA with *C. odorata*-derived polyphenols not only enhances its antimicrobial activity but also imparts antioxidant and anti-inflammatory functionalities [10]. This multifunctionality is particularly advantageous for preventing implant-associated infections, promoting tissue integration, and ensuring the long-term stability and performance of biomedical implants [5].

Building upon this foundation, recent studies specifically focusing on the antibacterial efficacy of *C. odorata* underscore its potential as a natural alternative to conventional antibiotics for infection control. Incorporating phytochemicals from medicinal plants into bioceramic matrices thus presents a promising strategy to enhance the antimicrobial performance of biomedical devices. In this study, the phytochemical composition of *C. odorata* extract was quantified, and *C. odorata*-doped nanoporous hydroxyapatite was synthesized. The doped hydroxyapatite was characterized by X-ray diffraction (XRD) for phase identification and Fourier Transform Infrared (FTIR) spectroscopy for functional group analysis [4]. The antimicrobial properties of the materials were evaluated using agar diffusion method, to measure inhibition zones against *Staphylococcus aureus (S. aureus)*.

Materials and methods

Preparation of plant extract
C. odorata leaves were harvested from the Pauh Putra Main Campus of Universiti Malaysia Perlis. The leaves were meticulously washed with distilled water to remove any dirt. Following the cleaning process, the leaves were oven-dried at 40 °C for 48 hours. Once dried, the leaves were finely ground using an electric grinder and passed through a 200-micron mesh sieve. For the extraction process, 30 g of the powdered C. odorata leaves were subjected to Soxhlet extraction with methanol and ethanol as solvents, corresponding to their respective boiling points of 64.7 °C and 78.37 °C in a water bath. The filtrate was separated from residue via Whatman filter paper no. 1 and then, using rotary evaporator, partial evaporation was done at 40 °C. The concentrated extract was further dried in an oven at 40 °C until a crude extract was obtained. The crude extract was kept in refrigerator at 4 °C before further analysis.

Total phenolic content
A sample of *C. odorata* extract was prepared at a concentration of 10 mg/mL with distilled water. The crude was dissolved into distilled water using ultra-sonic bath sonicator. This procedure was similarly applied to the 80% ethanol crude extract. To determine the total phenolic content (TPC), the Folin-Ciocalteu (FC) colorimetric method was used. Initially, 0.1 mL of the 10 mg/mL 80% methanol extract was combined with 0.2 mL of FC reagent, followed by the addition of 8 mL of distilled water. The mixture was thoroughly stirred and incubated at room temperature for 3 minutes. Subsequently, 20% sodium carbonate was added to the solution, which was then placed inside a dark cabinet for 30 minutes. Absorbance measurements were taken using an ultraviolet-visible spectrophotometer at 765 nm. The phenolic content concentration of the sample was determined using the calibration curve and expressed as gallic acid equivalents (mg GAE/g).

Total flavonoid content
A 10 mg/mL sample of *C. odorata* extract was prepared for this analysis. The aluminum chloride method was used to determine the total flavonoid content of *C. odorata*. Initially, 2 mL of distilled water and.5 mL of the extract was mixed in a test tube. To this, 0.15 mL of 50% sodium nitrate was mixed with previous mixture was incubated at room temperature for 5 minutes. Next, 10% aluminum chloride was introduced, and the mixture was incubated for an additional 30 minutes at the dark cabinet. Absorbance measurements were taken at 415 nm using a spectrophotometer. The flavonoid content concentration was calculated using the calibration curve and expressed as quercetin equivalents (mg QE/g). All samples were prepared in triplicate, and the procedure was repeated for the *C. odorata* ethanol extract.

Antioxidant activity
For the antioxidant activity test, a 250 mL stock solution of 60 µM DPPH was prepared. Initially, 1.97 mg of DPPH powder was mixed in 50 mL of 95% ethanol to create a 1 mM DPPH stock solution. Subsequently, 15 mL of this 1 mM DPPH stock solution was combined with 235 mL of 95% ethanol to form a 250 mL sample solution. The plant extract was subjected to serial dilution to prepare the antioxidant test samples. Seven concentrations (5, 3.5, 2.5, 1.25, 0.625, 0.5, and 0.1 mg/mL) were prepared by measuring 200 µL of each concentration into separate test tubes. Each test tube then received 2,500 µL of the 60 µM DPPH solution. The mixtures were thoroughly shaken and incubated in the dark at room temperature for 30 minutes. For the control, 200 µL of 95% ethanol was used. The percentage of inhibition was measured using the formula in Equation 1.

$$DPPH\ RSA\ \% = \frac{(A_{control} - A_{sample})}{A_{control}} \times 100\ \%$$ 　　　　(Equation 1)

Synthesis of nanoporous HA
Nanoporous hydroxyapatite (HA) nanoparticles were created by dissolving 9.45 g of calcium nitrate tetrahydrate (Ca $(NO_3)_2 \cdot 4H2O$) in 100 mL of distilled water, then adding 3 g of triblock polymer P123 (BASF, USA). Using 60 mL distilled water in different beaker, 3.17 g of diammonium hydrogen phosphate (($(NH_4)_2HPO_4$) was added to dissolve. This phosphate solution was then added dropwise to the surfactant-calcium solution under constant stirring, resulting in a milky mixture. To maintain an alkaline pH of 11, 1 M sodium hydroxide was gradually introduced. The mixture was left on lab desk for 24 hours with covered parafilm. The excess surfactant was removed from the precipitate through a series of washing for 5 times and centrifugation steps at 3,000 rpm for 20 minutes. The suspended precipitate was placed in a Petri dish and dried in an oven at 40 °C for 24 hours. The remaining of residue after filtration was removed and grinded using mortar and pestle. Lastly, the grinded powder was transferred to muffle furnace.

Preparation of HA doped with *C. odorata* extract
Hydroxyapatite (HA) doped with *C. odorata* extract was prepared as follows: Initially, 3 g of HA powder was placed in a 100 mL conical flask. Subsequently, 50 mL of *C. odorata* extract at concentrations of 20 mg/mL was added to the flask, followed by agitation on a laboratory shaker for 24 hours to ensure uniform suspension of the HA powder. The resulting mixture was then filtered using filter paper to isolate the solid residue, which was subsequently dried in a vacuum oven for 24 hours. Once dried, the HA doped with *C. odorata* extract was finely ground using a mortar and pestle and stored in an airtight container until further use.

Characterisations of HA powder
The phases of the sample were identified through X-ray diffraction (XRD) analysis. Fourier Transform Infrared (FTIR) spectroscopy, spanning a wavenumber range of 400 cm^{-1} to 4000 cm^{-1}, was used to analyze the primary functional groups present in hydroxyapatite.

Agar diffusion method
The antimicrobial efficacy of HA-doped *C. odorata* extract pellets, prepared at concentrations of 20 mg/mL and 80 mg/mL, was assessed against *S. aureus* using the agar diffusion method. Triplicate samples of HA-doped *C. odorata* pellets at 20 mg/mL were incorporated into nutrient agar prior to solidification. As a positive control, 100 µL of a 50 mg/mL amoxicillin stock solution was applied to separate agar plates. Next, 100 µL of a standardized *S. aureus* inoculum was evenly spread across the agar surface using a sterile cotton swab. Incubation was done in incubator at 37 °C for 24 hours. After incubation, the inhibition zone diameters were measured with a Vernier caliper, and the area of the zones was calculated using Equation 2. The same experimental protocol was repeated for HA-doped *C. odorata* pellets at a concentration of 80 mg/mL.

$$Area\ of\ inhibition\ zone\ =\ Area\ of\ pellet\ +\ Inhibition\ zone\ -\ Area\ of\ pellet \quad \text{(Equation 2)}$$

Results and discussion

Total phenolic content, total flavonoid content, and antioxidant activity

The total phenolic content (TPC) of the extract was assessed using the Folin-Ciocalteu (FC) assay, with ethyl acetate fraction and gallic acid serving as the standard phenolic compound. The phenolic content concentration in the extract was then compared. According to the data in Table 1, the highest phenolic content was found in the 80% methanol extract of *C. odorata*, measuring 114.51 ± 4.63 mg GAE/g. In contrast, the TPC for the 80% ethanol extract of *C. odorata* was 58.68 ± 3.67 mg GAE/g.

Table 1. TPC concentration of 80% ethanol and 80% methanol *C. odorata* extract

Extraction Samples	TPC Concentration (mg GAE/g)
80% ethanol	58.68 ± 3.67
80% methanol	114.51 ± 4.63

Based on the concentrations of flavonoids in Table 2, the highest flavonoid content was also from 80% methanol *C. odorata* extract, which was 216.32 ± 3.98 mg QE/g, while the total flavonoid content of 80% ethanol *C. odorata* extract was 61.84 ± 2.13 mg QE/g.

Table 2. TFC concentration of 80% ethanol and 80% methanol *C. odorata* extract

Extraction Samples	TFC Concentration (mg QE/g)
80% ethanol	61.84 ± 2.13
80% methanol	216.32 ± 3.98

From the results, it can be determined that the methanol *C. odorata* extract has the highest concentration of phenolic and flavonoid content, which are 114.51 ± 4.63 mg GAE/g and 216.32 ± 3.98 mg QE/g, respectively. This is in accordance with Alabi *et al*. [11], where the phytochemical test of methanol *C. odorata* extract in their study exhibited the highest flavonoid and phenolic content compared to *C. odorata* ethanol extract. Methanol, with a boiling point of 64.7 °C, is preferred over ethanol, which has a boiling point of 78.4 °C, for extraction purposes. This is because methanol requires a lower temperature for solvent evaporation in the rotary evaporator, thereby reducing the risk of damaging the extract. Methanol also offers a higher extraction yield and greater concentration of bioactive compounds compared to ethanol. Additionally, due to its lower boiling point, methanol evaporates more easily after the extraction process, resulting in a higher yield of antioxidant components.

The DPPH assay operates on the principle of discoloration, where the violet color of the stable DPPH free radical solution turns yellow upon reduction. The DPPH scavenging activity values for 80% ethanol and 80% methanol *C. odorata* crude extracts are presented in Tables 3 and 4, respectively.

**Table 3.** DPPH scavenging activity of 80% ethanol *C. odorata* extract

Extract Concentration (mg/mL)	DPPH Scavenging Activity (%)
0.1	34.57 ± 7.43
0.5	50.79 ± 2.95
0.625	63.67 ± 2.39
1.25	64.90 ± 1.86
2.5	69.31 ± 0.53
3.5	71.43 ± 0.53
5	73.54 ± 0.53

Table 4. DPPH scavenging activity of 80% methanol *C. odorata* extract

Extract Concentration (mg/mL)	DPPH Scavenging Activity (%)
0.1	58.42 ± 1.78
0.5	65.02 ± 7.69
0.625	79.21 ± 1.78
1.25	81.19 ± 1.98
2.5	82.84 ± 2.06
3.5	87.79 ± 0.57
5	88.94 ± 1.03

Based on the results, 80% methanol *C. odorata* extract at 5 mg/mL concentration exhibited the highest antioxidant activity (88.94%) compared to 80% ethanol *C. odorata* extract at the same concentration (73.54%). As determined by Azmi *et al*. [12], the methanol extract has a high percentage of DPPH scavenging radical (21.26%) compared to the ethanol extract (8.8%). Both results also indicated that the higher the extract concentration, the lower the absorbance value. A lower absorbance value will increase the DPPH scavenging activity.

X-ray diffraction

The XRD pattern of the synthesized HA shown in Figure 1 aligns with the standard HA diffraction pattern, identified by the PDF number 01-074-0565. The lattice constants are a = b = 9.4240 and c = 6.9019, with a hexagonal P63/m space group. The XRD pattern revealed three primary peaks at 2θ values of 25.95°, 32.01°, and 33.03°, corresponding to the (002), (211), and (300) diffraction planes, respectively.
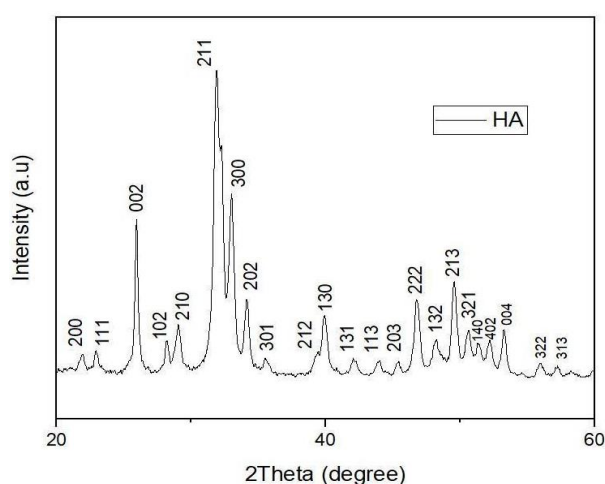
Figure 1. Results of XRD analysis

Fourier transform infrared spectroscopy

The functional groups present in the prepared samples can be described by the infrared spectra. Figure 2 shows the FTIR analysis of the synthesized HA sample. The mid-IR spectrum (400–4000 cm^{-1}) is the most widely used spectrum for FTIR analysis. The band appearing at 3569 cm^{-1} represents OH$^-$. The wavelength at 2886 cm^{-1} represents the C–H stretching bond. The peak at 1416 cm^{-1} indicates the CO_3^{2-} functional group, while the absorption peak at 1030 cm^{-1} corresponds to the PO_4^{3-} functional group. The FTIR analysis for HA was obtained from [1]. Figure 2 shows the results of FTIR analysis for HA, HA doped with 80% methanol *C. odorata* extract at 20 mg/mL concentration, and HA doped with 80% methanol *C. odorata* extract at 80 mg/mL concentration. From the FTIR results for HA with 20 and 80 mg/mL of extract, the functional group of PO_4^{3-} remained in the sample. The peaks for OH$^-$, C–H, and CO_3^{2-} can be slightly observed compared to the HA sample. There were no new absorption peaks for both HA samples with different *C. odorata* extract concentrations.
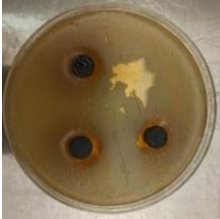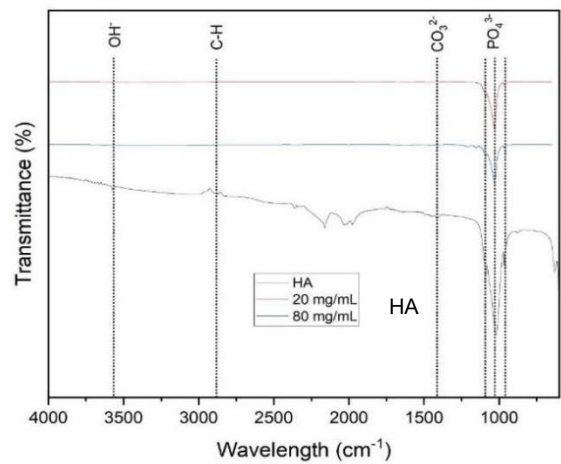
Figure 2. Results of FTIR analysis

Antimicrobial assay

From Table 5, it can be observed that HA-doped *C. odorata* extract pellets at 80 mg/mL concentration have the largest inhibition zone (106 mm^2) compared to the pellets at 20 mg/mL concentration (48 mm^2).

Table 5. Inhibition zone for different concentrations of HA-doped *C. odorata* extract pellets

Extract Concentration (mg/mL)	Density of bacteria (10^4)	Inhibition Zone (mm^2)
20		48
80		106

According to Truong et al. [12], methanol is the optimal solvent for antibacterial extraction, with ethanol and hexane as alternatives. This study is in line with [5], who demonstrated that methanol and ethanol are highly effective extraction solvents for antibacterial studies due to their strong antibacterial activity against pathogens. The antibacterial activity of the pellets could also be influenced by the presence of bioactive compounds in *C. odorata* extract [13]. The antimicrobial assay demonstrated a concentration-dependent inhibitory effect of HA-doped *C. odorata* extract pellets against the tested bacteria. The inhibition zone increased significantly with higher extract concentrations, where the 80 mg/mL sample exhibited the largest inhibition zone (106 mm²) compared to the 20 mg/mL sample (48 mm²). This suggests that the bioactive compounds present in *C. odorata* contribute effectively to the antimicrobial activity when incorporated into the HA matrix. The enhanced antimicrobial performance at higher concentrations may be attributed to the increased availability of phytochemicals such as flavonoids and phenolics, known for their antibacterial properties. These findings highlight the potential of *C. odorata*-loaded HA as a promising biomaterial for applications requiring infection control.

Conclusion

In this study, 80% methanol *C. odorata* extract exhibited better antioxidant activity than 80% ethanol *C. odorata* extract. The TPC and TFC tests also showed that the methanol extract has the highest concentration of phenolic and flavonoid contents compared to the ethanol extract. There was a relationship between the concentration of methanol *C. odorata* extract and its antimicrobial activity against *S. aureus*. The XRD analysis of HA indicated three main peaks at 2θ = 25.95°, 32.01°, and

33.03°, which correspond to the diffraction planes of (002), (211), and (300), respectively. The results for the analysis of nanoporous HA confirmed the presence of OH^-, C–H, CO_3^{2-}, and PO_4^{3-} functional groups. The FTIR analysis of HA-doped *C. odorata* extract showed that there was a reduction in peak intensity for both concentrations of HA-doped *C. odorata* powder in comparison with the synthesized HA. The antimicrobial activity of HA doped with 80% methanol *C. odorata* extract pellets against *S. aureus* revealed that the pellets at both concentrations (20 and 80 mg/mL) exhibited antimicrobial properties, as indicated by the area of inhibition zone. Due to the increase of drug-resistant pathogens, natural compounds from plants can serve as an alternative to fight bacterial infections in medical implants. Furthermore, *C. odorata* extract can be used as an alternative to synthetic antibiotics and drugs.

Acknowledgement

References

[1] N. F. Mohammad, F. S. A. Fadzli, S. S. M. Saleh, C. W. S. R. Mohamad, and M. A. A. Taib, "Antibacterial Ability of Mesoporous Carbonated Hydroxyapatite," in J. Phys. Conf. Ser., vol. 1372, no. 1, 2019, p.012081 doi: 10.1088/1742-6596/1372/1/012081.

[2] N. F. Mohammad, F. Y. Yeoh, N. P. Ling, and R. Othman, "Synthesis & Characterization of Mesoporous Hydroxyapatite by Co-Precipitation Method," in Asian International Conf. on Materials, Minerals and Polymer, 2012, pp. 626–633.

[3] N. F. Mohammad, R. Othman, and F. Yee-Yeoh, "Nanoporous hydroxyapatite preparation methods for drug delivery applications," Rev. Adv. Mater. Sci., vol. 38, no. 2, pp. 138–147, 2014.

[4] F. Liu et al., "Hydroxyapatite / silver electrospun fibers for anti-infection and osteoinduction," J. Adv. Res., vol. 21, pp. 91–102, 2020, doi: 10.1016/j.jare.2019.10.002.

[5] C. Bouvet, S. Gjoni, B. Zenelaj, B. A. Lipsky, E. Hakko, and I. Uçkay, "*Staphylococcus aureus* soft tissue infection may increase the risk of subsequent staphylococcal soft tissue infections," Int. J. Infect. Dis., vol. 60, pp. 44–48, 2017, doi: 10.1016/j.ijid.2017.05.002.

[6] C. R. Arciola, D. Campoccia, and L. Montanaro, "Implant infections: Adhesion, biofilm formation and immune evasion," Nat. Rev. Microbiol., vol. 16, no. 7, pp. 397–409, 2018, doi: 10.1038/s41579-018-0019-y.

[7] L. Wang, C. Hu, and L. Shao, "The-antimicrobial-activity-of-nanoparticles--present-situati," Int. J. Nanomedicine, vol. 12, pp. 1227–1249, 2017, [Online]. Available: https://www.ncbi.nlm.nih.gov/pmc/articles/PMC5317269/pdf/ijn-12-1227.pdf.

[8] N. F. Mohd Shamsuddin Tan, M. H. Zainal Abidin, L. I. Hussein, and M. H. Mokhtar, "Qualitative Phytochemical Analysis and Antibacterial Potential of *Chromolena odorata* Leaves as affected by Soxhlet and Maceration Extraction," J. Adv. Ind. Technol. Appl., vol. 1, no. 2, pp. 38–48, 2020, doi: 10.30880/ijie.2020.01.02.005.

[9] C. W. S. R. Mohamad, E. M. Cheng, and N. A. A. Talib, "Antibacterial Activity of Biodegradable Plastic from *Chromolaena odorata* (Pokok Kapal Terbang) Leaves," J. Phys. Conf. Ser., vol. 2071, no. 1, p. 012010, 2021, doi: 10.1088/1742-6596/2071/1/012010.

[10] A. Sirinthipaporn and W. Jiraungkoorskul, "Wound Healing Property Review of Siam Weed, *Chromolaena odorata*," Pharmacogn. Rev, vol. 1, no. 21, pp. 35–38, 2017, doi: 10.4103/phrev.phrev_53_16.

[11] M. A. Alabi, O. Olusola-Makinde, and M. K. Oladunmoye, "Evaluation of Phytochemical Constituents and Antibacterial Activity of *Chromolaena odorata* L. Leaf Extract against Selected Multidrug Resistant Bacteria Isolated from Wounds," South Asian J. Res. Microbiol., no. January, no. 3, vol. 5, pp. 1–9, 2020, doi: 10.9734/sajrm/2019/v5i330132.

[12] D. H. Truong, D. H. Nguyen, N. T. A. Ta, A. V. Bui, T. H. Do, and H. C. Nguyen, "Evaluation of the use of different solvents for phytochemical constituents, antioxidants, and in vitro anti-inflammatory activities of *Chromolaena odorata*," J. Food Qual., pp. 1-9, 2019, doi: 10.1155/2019/8178294.

[13]   S. N. A. Azmi, C. W. S. R. Mohamad, and K. F. Kasim, "Encapsulation of *C. odorata* extracts for antimicrobial activity," J. Phys. Conf. Ser., vol. 1372, no. 1, pp. 012046, 2019, doi: 10.1088/1742-6596/1372/1/012046.

[14]   P. O. Omeke, J. O. Obi, N. A. I. Orabueze, and A. C. Ike, "Antibacterial activity of leaf extract of *Chromolaena odorata* and the effect of its combination with some conventional antibiotics on *Pseudomonas aeruginosa* isolated from wounds," J. Appl. Biol. Biotechnol., vol. 7, no. 3, pp. 36–40, 2019, doi: 10.7324/JABB.2019.7